Supplementary Information for

The structure of POMGNT2 provides new insights into the mechanism to determine the functional *O*-mannosylation site on α-dystroglycan

Rieko Imae, Naoyuki Kuwabara, Hiroshi Manya, Tomohiro Tanaka, Masato Tsuyuguchi, Mamoru Mizuno, Tamao Endo, and Ryuichi Kato

Corresponding authors:
Ryuichi Kato, Ph. D.
E-mail: ryuichi.kato@kek.jp
Tamao Endo, Ph. D.
E-mail: endo@tmig.or.jp

This PDF file includes:

Supplementary Information Text

Materials

The structures of synthesized mannosyl peptide used in this work (Table 1) were identified by matrix-assisted laser desorption ionization time-of-flight mass spectrometry (MALDI-TOF MS).

379Man-long: Ac-TIRTRGAIIQT(Man)PTLGPIQPTR-NH_2

Found *m/z* 2493.8 $[M+H]^+$, calculated *m/z* 2493.4 $[M+H]^+$.

379Man-short: Ac-QT(Man)PTLGPIQPTR-NH_2

Found: *m/z* 1511.4 $[M+H]^+$, calculated *m/z* 1511.8 $[M+H]^+$.

Methods

Protein expression and purification

For large-scale expression and purification, we generated a stable line of HEK293S GnT- (ATCC CRL-3022) cells that expressed protein A-fused bovine sPOMGNT2. After inoculation of the stable cell line for 2–3 weeks, the medium containing secreted protein A-fused sPOMGNT2 was precipitated by ammonium sulfate and solubilized by PBS containing 0.05% NP-40. The suspension solution was subjected to IgG affinity column chromatography (GE Healthcare). After protein A tag removal by TEV protease digestion, sPOMGNT2 was further purified by MonoQ anion exchange column chromatography (GE Healthcare). Sugar chains of sPOMGNT2 were removed by Endo Hf glycosidase (New England Biolabs), overnight at room temperature, followed by amylose resin purification (New England Biolabs) and Superdex 200 increase gel filtration (GE Healthcare). Purified sPOMGNT2 was solubilized in 10 mM HEPES (pH 7.5), 150 mM NaCl, 1 mM DTT, and 10 mM $MgCl_2$.

Crystallization and structure determination

Purified sPOMGNT2 was subjected to initial crystallization screening using an automated protein crystallization and monitoring system [1]. Subsequent optimization of conditions was carried out by hanging-drop vapor diffusion by mixing equal volumes of protein and reservoir solutions.

Crystals of the UDP-bound form of sPOMGNT2 were obtained in 0.1M Tris-HCl

(pH 8.0 or 8.5), 12%–16% PEG 8,000 and 1% tacsimate (pH 7.0) (Hampton Research) at 277 K. Before X-ray diffraction experiments, the crystals were soaked in reservoir solution containing an additional 25% ethylene glycol as a cryo-protectant. Initial phase determination was performed by the iodide–SAD (single wavelength anomalous dispersion) method using a wavelength of 1.9000 Å at beamline BL-1A (Photon Factory, KEK, Tsukuba, Japan) at 100 K. Crystals for that purpose were prepared by soaking in 0.25 M KI for 30 min at 277 K. Crystals of the mannosyl peptide-bound forms were obtained by soaking with 12.5 mM of each mannosyl peptide for 0.5–3 hr at 277 K. X-ray diffraction data of native and peptide soaked crystals were collected at beamlines BL-1A, BL-17A (Photon Factory, KEK) and P14 (PETRA III, EMBL).

Collected X-ray diffraction data were integrated by XDS [2] and scaled using aimless in the CCP4i software package [3]. Mannosyl-peptide complex crystal structures were solved by Phenix.Phaser, using the UDP-bound structure as a search model. Structure refinement was performed by Coot [4] and phenix.refine [5]. Data collection and refinement statistics are summarized in Supplemental Table 1. Figures of crystal structures were made by the PyMOL Molecular Graphics System (Schrödinger, LLC). Hydrogen bonds and hydrophobic interactions were calculated by Ligplot [6].

Generation of sPOMGNT2 mutants

The expression vector for the secreted type of human sPOMGNT2 (Arg24 to the C-terminus) was prepared by inserting the PCR product into the EcoRI and XhoI sites of ss1-His/Myc-pcDNA3.1 [7]. For the truncated mutants (T445Δ and R477Δ), the PCR products encoding Arg24 to Thr445 and Arg24 to Arg477, respectively, were inserted into the same site of the vector. Each point mutation was introduced by the quick change PCR method (Agilent Technologies) or using In-Fusion cloning techniques (Clontech).

Enzymatic assay for sPOMGNT2

The secreted type of wild-type (WT) or mutant sPOMGNT2 (Arg24 to the C-terminus) was expressed in HEK293T cells using Lipofectamine 3000 (Life Technologies Japan). The expressed proteins were immunoprecipitated from the culture supernatant, except where otherwise indicated, with anti-c-Myc antibody-agarose (rabbit polyclonal; Sigma). The proteins bound to the agarose were quantified by Western blotting and used

as the enzyme sources. Enzymatic reactions of the WT or mutant sPOMGNT2 were performed in 20 μL of reaction buffer (100 mM MOPS-NaOH, pH 7.0, 0.5% Triton X-100) containing 10 mM $MnCl_2$, 10 mM $MgCl_2$, 250 μM UDP-GlcNAc, 50 μM acceptor peptide and the enzyme-bound agarose (66.7 ng protein) at 37°C for 4 hr, except where otherwise indicated. For measuring the enzymatic activity of the mutant sPOMGNT2, the 379Man long peptide was used as an acceptor peptide. Because the R158H, N163A and R445Δ mutants were scarcely secreted to the culture media, cell lysates were prepared using PBS buffer containing 0.5% Triton X-100 and protease inhibitor cocktail (Nacalai Tesque), and the expressed proteins were immunoprecipitated with anti-c-Myc antibody-agarose. Then, sPOMGNT2 enzymatic reactions were performed as described above except that the enzyme-bound agarose (70.6 ng protein) was used and the incubation time was 6 hr. For the assays to examine the divalent cation requirements, a reaction buffer containing divalent cations (10 mM $MnCl_2$ and 10 mM $MgCl_2$) or 10 mM EDTA, 250 μM UDP-GlcNAc, 50 μM acceptor peptide (379Man long) and the enzyme-bound agarose was used. For the kinetic experiments, enzymatic reactions were performed in the reaction buffers containing 10 mM $MnCl_2$, 10 mM $MgCl_2$, 20 mM UDP-GlcNAc, 0.1, 1, 2, 5, or 10 mM acceptor peptide (379Man long or short) and the enzyme-bound agarose at 37 °C for 2 hr. Each product was analyzed by reversed-phase HPLC as described previously [7]. Each enzymatic activity was calculated from the product peak area. The kinetic parameters were obtained by non-linear regression (Michaelis-Menten equation) using SigmaPlot 14.0 (Hulinks).

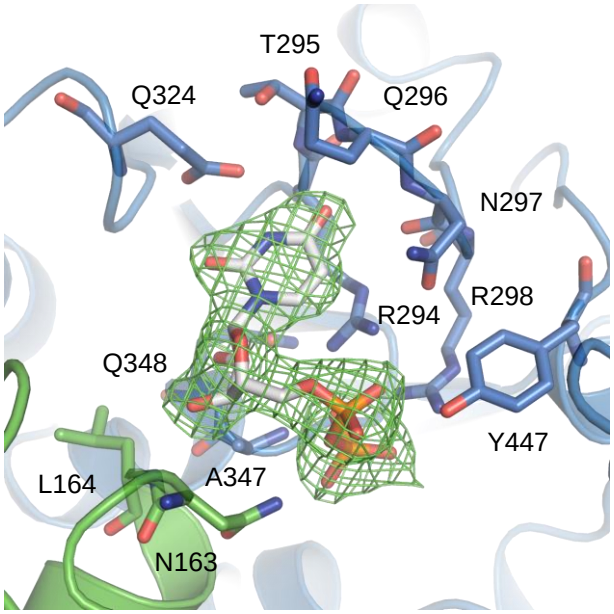

Fig. S1.

Omit map of the UDP molecule of the sPOMGNT2-UDP complex. The contour level is 4.0 σ.

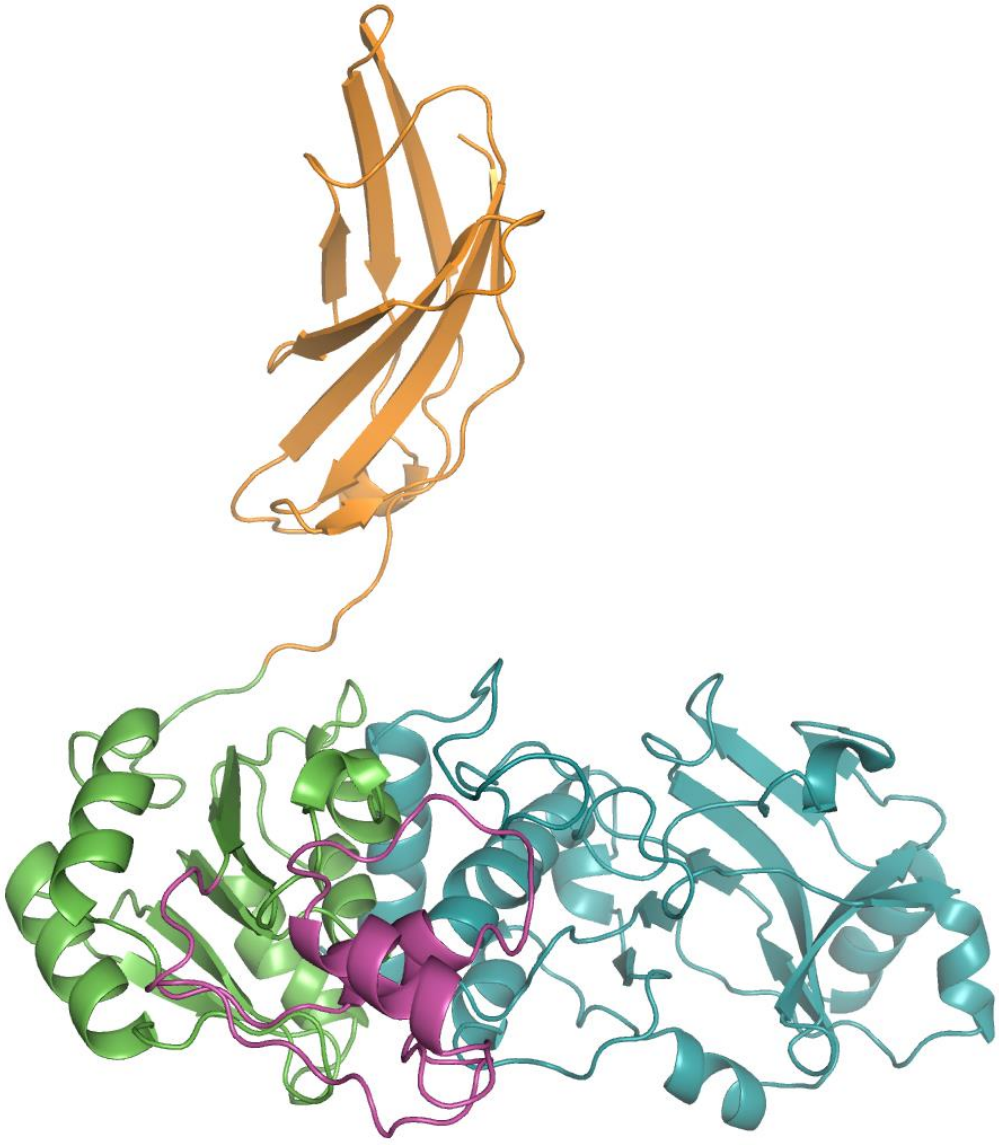

Fig. S2.

Domain organization of the sPOMGNT2 monomer. The unique insertion region (residues 395–451) in the C-lobe is colored purple. The N-lobe, C-lobe and C-terminal FnIII domain are colored blue, green, and orange, respectively.

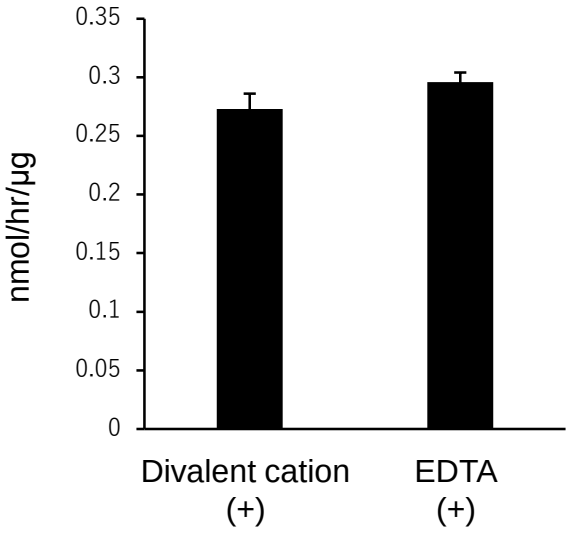

Fig. S3.

Divalent cation requirements for the enzymatic activity of sPOMGNT2. A reaction buffer containing divalent cations (10 mM $MnCl_2$ and 10 mM $MgCl_2$) or 10 mM EDTA was used. sPOMGNT2 immunoprecipitated from the culture media was used for the enzyme reaction. Average values ± SE of three independent experiments are shown.

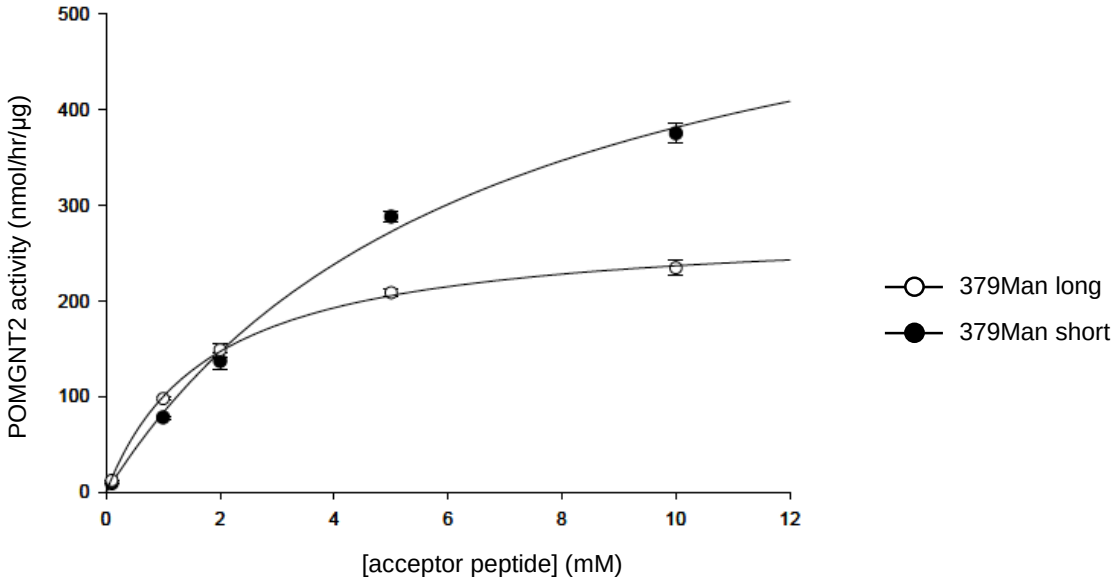

Fig. S4.

Kinetic analysis of sPOMGNT2. POMGNT2 activity was measured with increasing amounts of the 379Man long peptide (open circles) or 379Man short peptide (closed circles). Average values ± SE of three independent experiments are shown.

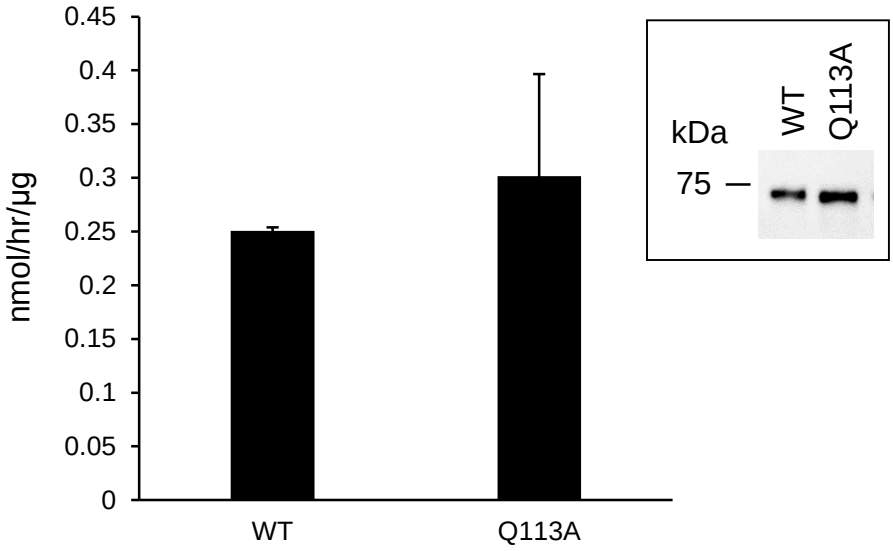

Fig. S5.

Enzymatic activities of the WT and Q113A mutant of sPOMGNT2. sPOMGNT2 immunoprecipitated from the culture media was used. Inset: immunoblot analysis of sPOMGNT2 proteins to normalize input sPOMGNT2. Average values ± SE of three independent experiments are shown.

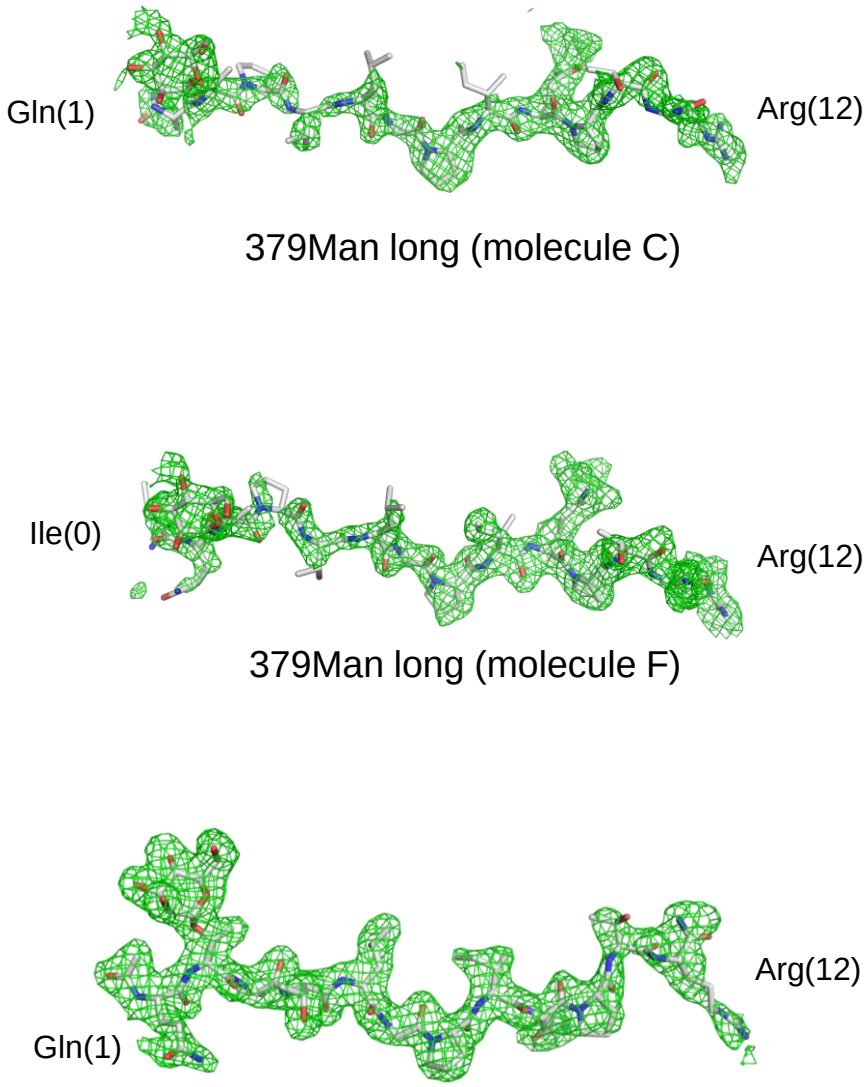

Fig. S6.

Omit maps of mannosyl peptides in sPOMGNT2 complexes. In the case of 379Man long peptides, conformers 1 are shown. The contour level is 2.5 σ.

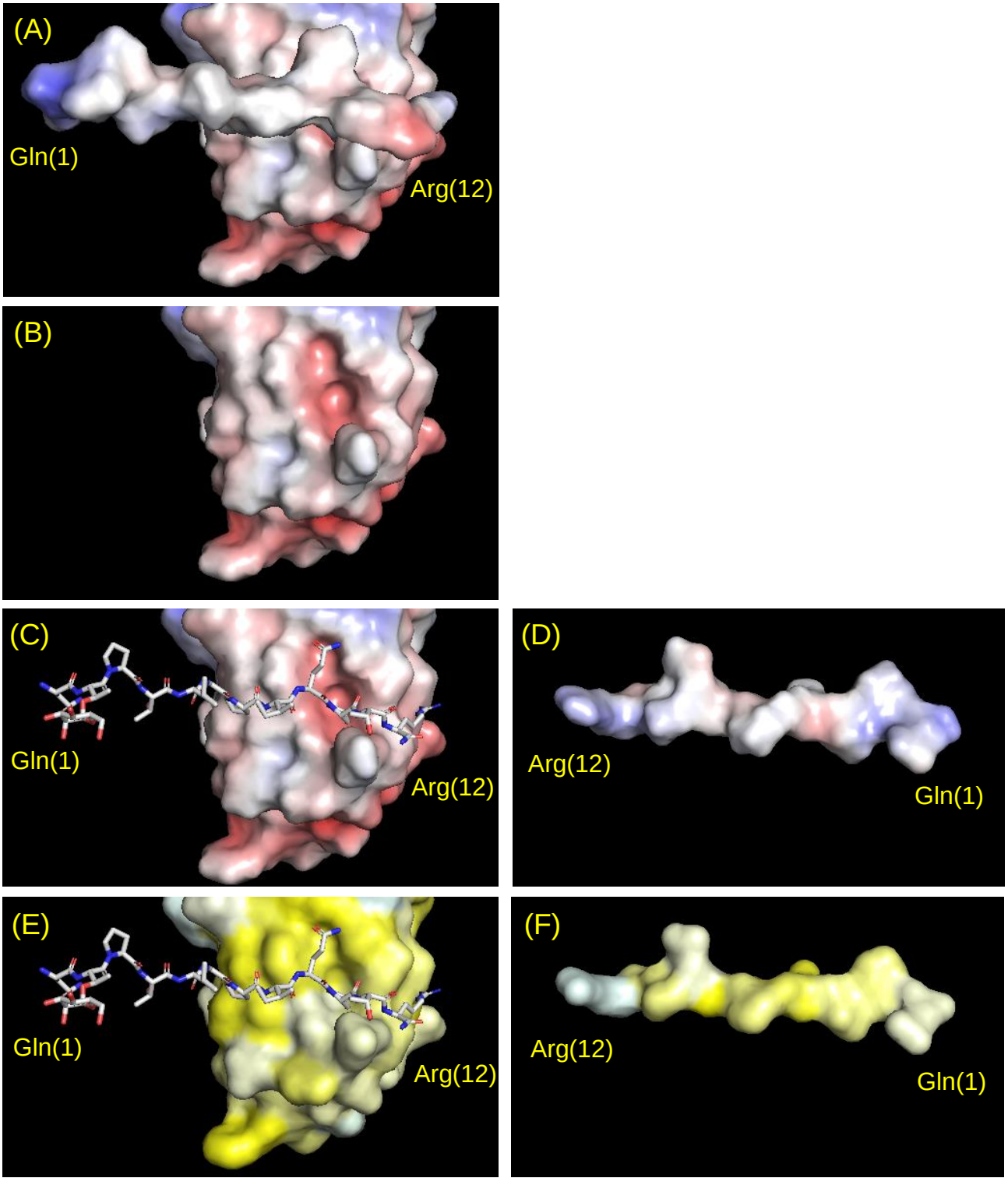

Fig. S7.

Models of the molecular surfaces of sPOMGNT2 and the 379Man short peptide in the complex. Only the FnIII domain of sPOMGNT2 is shown. (A) Surface charge of the peptide complex. Red and blue show acidic and basic, respectively. (B) Surface charge of sPOMGNT2 after removing the peptide molecule from the complex. (C) Surface charge of sPOMGNT2 and stick model of the peptide. (D) Surface charge of the peptide which is shown by an open book orientation of panel C. (E) Surface hydrophobicity of sPOMGNT2 and stick model of the peptide. Hydrophobicity is shown in yellow. (F) Surface hydrophobicity of the peptide which is shown by an open book orientation of panel E.

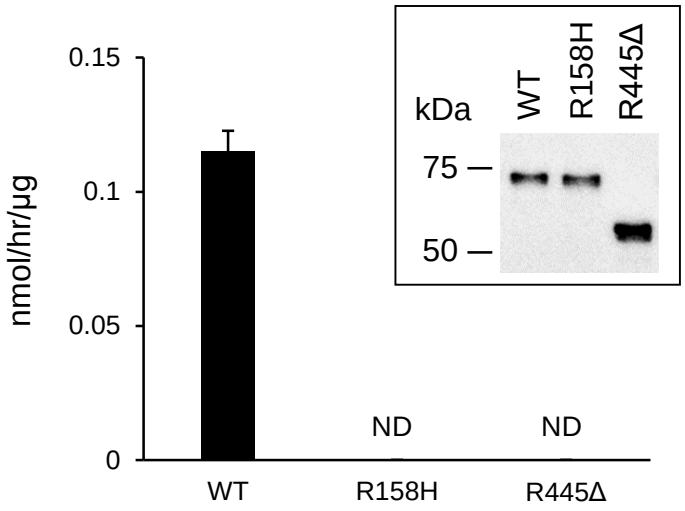

Fig. S8.

Enzymatic activities of the WT and disease-related mutants of sPOMGNT2. sPOMGNT2 immunoprecipitated from the cell lysate was used because the R158H and R445Δ mutants were scarcely secreted to the culture media. Inset: immunoblot analysis of sPOMGNT2 proteins to normalize input sPOMGNT2. ND means that the activities were not detected. Average values ± SE of three independent experiments are shown.

	A	317 T	Man	P	T	P	V	T	A	I	G	P	P
	P	319 T	Man	P	V	T	A	I	G	P	P	T	T
	Q	379 T	Man	P	T	L	G	P	I	Q	P	T	R
	1	2		3	4	5	6	7	8	9	10	11	12
379Man short	R438	N160 **C437**	**H166** **H166** **C436**	**H125** **H125** **F159** F247	**H125** T127	N126	N126 N126	L557 **W559** V575	**W559**	W525 **W559** F572	Q527 N532 T533 Y534	N532 N532	N532 N532 T533 Y534
379Man long (C)	N160 D162 D162 W197	N160 **C437**	**H166** **H166**	**H125** **H125** **F159** F247	**H125** T127	**H125** N126	N126 N126	**W559** V575		**W559**	Q527 N532	N532 N532	N532 N532 T533 Y534
379Man long (F)	N160 D162 W197	**C437**	**H166** **H166** Y245 **C436**	**H125** **H125** **F159** F247	**H125** T127	**H125** N126 F247	N126 N126	**W559**	**W559**	W525 **W559**	Q527 N532 **W559**	N532 N532	N532 T533 Y534
	catalytic domain							FnIII domain					

Fig. S9.

Summary of the interaction between sPOMGNT2 and mannosyl peptides. The top three columns show the sequences of α-DG at around Thr317, Thr319, and Thr379, respectively. The bottom three columns show interacting amino acid residues of sPOMGNT2 in the peptide complex structures. The residues which interact with the peptides by hydrogen bonds, hydrophobic interactions and CH-π interactions are presented by red, black and purple letters, respectively. Bold and underlined residues indicate that the mutants lost or almost lost their activities, and underlined residues indicate that the mutants showed partially reduced activities.

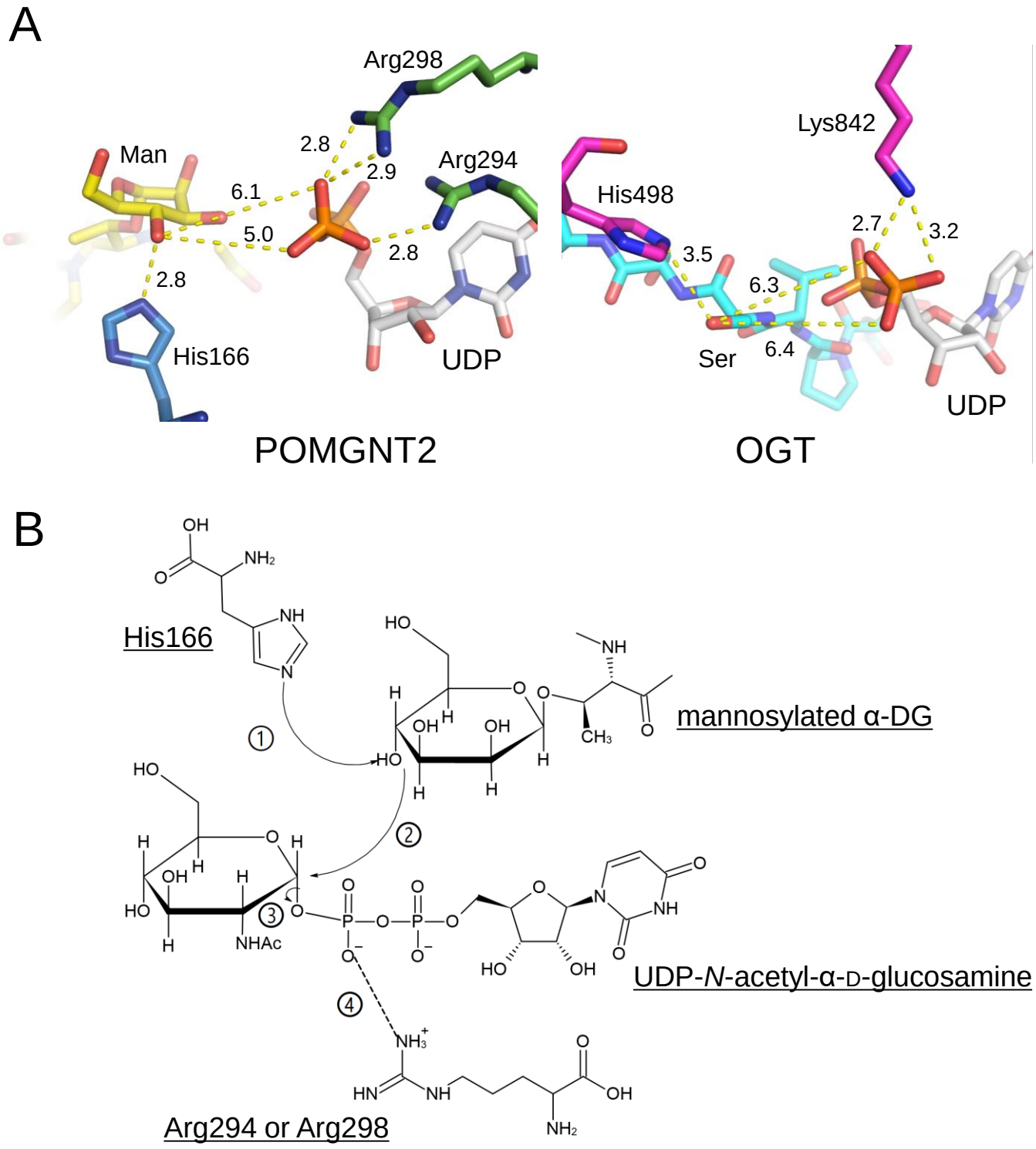

Fig. S10.

(A) Catalytic active sites of POMGNT2 (left) and OGT (right). Numbers are distances between the two respective atoms (Å, indicated by broken yellow lines). (B) Proposed enzymatic mechanism of POMGNT2. The ordered sequential bi-bi kinetic mechanism (steps 1~4) is shown based on the crystal structure and comparison of OGT. His166 is the proposed catalytic base. Arg294 and/or Arg298 stabilizes the UDP moiety.

Table S1.
Data collection and refinement Statistics

	sPOMGNT2	sPOMGNT2 soaked with NaI	sPOMGNT2 in complex with 379Man long peptide	sPOMGNT2 in complex with 379Man short peptide
data collection statistics				
beamline	PF, BL17A	PF, BL1A	PETRA III, P14	PF, BL1A
Wavelength (angstrom)	1.0718	1.9000	0.9763	1.1000
Resolution range (angstrom)	49.30-2.40 (2.47-2.40)	49.63-2.86 (3.01-2.86)	49.57-2.05 (2.09-2.05)	48.29-2.10 (2.14-2.10)
Space group	$P2_12_12_1$	$P2_12_12_1$	$P2_1$	$P2_12_12_1$
Unit cell a,b,c (angstrom)	96.1, 106.2, 132.4	95.9, 107.0, 132.7	86.2, 104.4, 148.6 beta=90.1	92.39, 104.44, 126.84
Total reflections	717530	2557614	576568	1004986
Unique reflections	53742	32270	163077	72133
Multiplicity	13.4	79.3	3.5	13.9
Completeness*	100.0 (100.0)	100.0 (100.0)	99.0 (99.0)	99.8 (96.7)
Mean I/sigma(I)*	10.5 (1.6)	12.8 (1.3)	10.8 (1.6)	16.0 (1.9)
Wilson B-factor	42.4	38.3	30.8	32.2
R-merge*	0.247 (1.858)	0.824 (8.235)	0.070 (0.801)	0.114 (1.574)
R-meas*	0.256 (1.913)	0.829 (8.292)	0.083 (0.945)	0.119 (1.631)
R-pim*	0.070 (0.518)	0.129 (1.322)	0.044 (0.497)	0.044 (0.582)
CC1/2*	0.997 (0.422)	0.994 (0.401)	0.999 (0.761)	0.999 (0.791)
number of sites	-	28	-	-
figure of merit	-	0.248	-	-
refinement statistics				
Reflections used in refinement	53665		162767	72055
Reflections used for R-free	2771		7922	3481
R-work	0.1989		0.202	0.1855
R-free	0.2383		0.24	0.2339
Number of non-hydrogen atoms	8647		18493	9056
macromolecules	8290		16823	8329
ligands (Man-peptide, UDP and Tris)	114		566	164
solvent	243		908	465
Protein residues	1049		2111	1046
RMS(bonds)	0.007		0.003	0.008
RMS(angles)	0.85		0.55	0.88
Ramachandran favored (%)	96.7		98.13	98.07
Ramachandran allowed (%)	3.3		1.87	1.93
Ramachandran outliers (%)	0.00		0.00	0.00
Rotamer outliers (%)	0.00		0.05	0.00
Clashscore	6.82		2.56	3.59
Average B-factor	54.28		40.9	50.08
macromolecules	54.48		39.72	50.01
ligands	60.51		61.11	50.23
solvent	44.55		42.6	46.08

*Statistics for the highest-resolution shell are shown in parentheses.

Table S2.

Hydrogen bonds between amino acid side chains of sPOMGNT2 and UDP

residue	atom	UDP atom	distance (Å)	
			chain A	chain B
Asn163	ND2	O1B	3.01	3.18
	ND2	O3A	2.90	3.41
Arg294	NH2	O2A	2.97	3.33
	NH1	O2B	2.78	2.86
Arg298	NH2	O3B	2.62	2.72
	NH2	O2A	3.46	3.68
	NH1	O2B	2.97	3.67
	NH1	O3B	3.27	2.93
Glu324	OE1	N3	2.81	3.28
Tyr447	OH	O2A	2.91	2.72

Table S3.

Hydrogen bonds between main chain atoms of sPOMGNT2 and UDP

residue	atom	UDP atom	distance (Å)	
			chain A	chain B
Leu164	N	O3'	2.94	2.91
Thr295	N	O4	3.49	3.69
Gln296	N	O4	2.81	2.97
Asn297	N	N	3.16	3.16
Ala347	N	O1B	3.40	3.16
	N	O2B	2.93	3.19
Gln348	N	O2'	3.85	3.85

Table S4.

Molecule names in each asymmetric unit

	sPOMGNT2	mannosyl peptide
non peptide	A, B	
379Man short	A, B	C
379Man long	A, B, D, E	C (conformer 1 and 2) F (conformer 1 and 2)

Occupancies of conformers 1 and 2 are 50%, respectively.

Table S5.

Structural comparison among sPOMGNT2 and its peptide complexes

	no peptide	379Man short	379Man long (A, B)	379Man long (D, E)
no peptide				
379Man short	0.393			
379Man long (A, B)	0.998	0.774		
379Man long (D, E)	1.041	0.766	0.178	

The r.m.s.d. values of Cα carbon of the sPOMGNT2 dimer among the structures are shown (Å). Since the 379Man long complex contains four protomers (two dimers) in the asymmetric unit, the calculation was carried out for each dimer.

Table S6.

Interactions between the catalytic domain of sPOMGNT2 and 379Man short peptide

Mannosyl peptide		sPOMGNT2		interaction	distance (Å)
residue	atom	residue	atom		
Mannose	O4	His166	NE2	hydrogen bond	2.76
	C4		NE2	hydrophobic	3.5
	C6	Cys436	SG	hydrophobic	3.5
Gln(1)	CD	Arg438	NH2	hydrophobic	3.5
	NE2		NH2	hydrophobic	3.1
Thr(2)	OG1	Asn160	OD1	hydrophobic	3.5
	CG2	Cys437	SG	hydrophobic	3.6
Pro(3)	O	His125	NE2	hydrogen bond	2.86
	C		NE2	hydrophobic	3.6
	O		CE1	hydrophobic	3.6
		Phe159		CH-π	3.6
	O	Phe247	CE1	hydrophobic	3.4
	O		CZ	hydrophobic	3.5
Thr(4)	O	His125	CE1	hydrophobic	3.6
	O	Thr127	CG2	hydrophobic	3.6
Leu(5)	CA	Asn126	OD1	hydrophobic	3.4
	C		OD1	hydrophobic	3.6
Gly(6)	N	Asn126	OD1	hydrogen bond	2.84
	O		ND2	hydrogen bond	3.03
	N		CG	hydrophobic	3.6

Interactions between the catalytic domain of sPOMGNT2 and 379Man short peptide are listed by LigPlot analysis. Distances of the hydrophobic and CH-π interactions were measured by PyMol, and the interactions at distances shorter than 3.7 Å are summarized in this table. The sPOMGNT2 residues to which the mutations were introduced are underlined.

Table S7.

Interactions between the FnIII domain of sPOMGNT2 and 379Man short peptide

Mannosyl peptide		sPOMGNT2		interaction	distance (Å)
residue	atom	residue	atom		
Pro(7)	CB	Leu557	CD2	hydrophobic	3.6
	O	Trp559	CH2	hydrophobic	3.3
	CD	Val575	CG1	hydrophobic	3.6
	CG		CG1	hydrophobic	3.6
Ile(8)	O	Trp559	CZ2	hydrophobic	3.6
Gln(9)	NE2	Trp525	CZ2	hydrophobic	3.5
		Trp559		CH-π	3.4
	OE1	Phe572	CD2	hydrophobic	3.6
Pro(10)	CD	Gln527	OE1	hydrophobic	3.3
	CA	Asn532	OD1	hydrophobic	3.2
	C		OD1	hydrophobic	3.3
	CB		C	hydrophobic	3.5
	CB	Thr533	N	hydrophobic	3.5
	CG	Tyr534	CD1	hydrophobic	3.4
Thr(11)	N	Asn532	OD1	hydrogen bond	2.57
	OG1		ND2	hydrogen bond	2.26
	CA		OD1	hydrophobic	3.5
	N		CG	hydrophobic	3.6
	OG1		CG	hydrophobic	3.1
Arg(12)	N	Asn532	O	hydrogen bond	2.91
	CA		O	hydrophobic	3.0
	CG	Thr533	OG1	hydrophobic	3.4

Interactions between the FnIII domain of sPOMGNT2 and 379Man short peptide are listed by LigPlot analysis. Distances of the hydrophobic and CH-π interactions were measured by PyMol, and the interactions at distances shorter than 3.7 Å are summarized in this table. The sPOMGNT2 residues to which the mutations were introduced are underlined.

SI References

1. R. Kato, *et al.*, A fully automated crystallization apparatus for small protein quantities. *Acta Crystallogr. F Struct. Biol. Commun.* **77**, 29–36 (2021).
2. W. Kabsch, XDS. *Acta Crystallogr. D Biol. Crystallogr* **66**, 125–132 (2010).
3. M. D. Winn, *et al.*, Overview of the CCP4 suite and current developments. *Acta Crystallogr. D Biol. Crystallogr.* **67**, 235–242 (2011).
4. P. Emsley, B. Lohkamp, W. G. Scott, K. Cowtan, Features and development of Coot. *Acta Crystallogr. D Biol. Crystallogr.* **66**, 486–501 (2010).
5. D. Liebschner, *et al.*, Macromolecular structure determination using X-rays, neutrons and electrons: recent developments in Phenix. *Acta Crystallogr. D Biol. Crystallogr.* **75**, 861–877 (2019).
6. A. C. Wallace, R. A. Laskowski, J. M. Thornton, LIGPLOT: a program to generate schematic diagrams of protein-ligand interactions. *Protein Eng.* **8**, 127–134 (1996).
7. M. Kanagawa, *et al.* Identification of a post-translational modification with ribitol-phosphate and its defect in muscular dystrophy. *Cell Rep.* **14**, 2209–2223 (2016).